Journal of Chromatography, 483 (1989) 63–84
Elsevier Science Publishers B.V., Amsterdam — Printed in The Netherlands

CHROM. 21 888

PREPARATIVE HIGH-PERFORMANCE LIQUID CHROMATOGRAPHY UNDER ISOCRATIC CONDITIONS

I. CRAIG SIMULATIONS FOR HEAVILY OVERLOADED SEPARATIONS

L. R. SNYDER* and J. W. DOLAN
LC Resources Inc., 3182C Old Tunnel Road, Lafayette, CA 94549 (U.S.A.)
and
G. B. COX
Medical Products Department, E. I. du Pont de Nemours Inc., Glasgow, DE 19701 (U.S.A.)
(First received May 10th, 1989; revised manuscript received August 15th, 1989)

SUMMARY

Craig simulations of preparative high-performance liquid chromatography were carried out for heavily overloaded separations as a function of the separation conditions (small-sample retention and column efficiency, sample size). These data were used to derive conditions for a maximum production rate (grams per hour) of purified product, and the results were compared with the treatment of Knox and Pyper. There is an optimum sample size and column plate number for every separation; these optimum conditions are related to the desired recovery of purified product and to the retention (capacity factor, k'; separation factor, α) of a small sample under the same chromatographic conditions.

Relative to the case of a 99.8% recovery of purified product from the feed, a 3-fold higher production rate is possible if sample size and column plate number are adjusted for 95% recovery of pure product; a 10-fold higher production rate is possible for conditions that give a 50% recovery of pure product. The required (optimum) plate number is halved on going from touching-band (99.8% recovery) separation to 95% recovery, and further halved for 50% recovery *vs.* 95% recovery. The maximum production rate also varies with sample retention (k', α for a small sample); a maximum value of α is preferred and k' should be between 0.5 and 3.

INTRODUCTION

The last 5 years have witnessed a dramatic expansion in our understanding of preparative high-performance liquid chromatography (HPLC) carried out under isocratic elution conditions[1–18]. The next major challenge is to digest this large mass of information and render it usable by practical workers. Knox and Pyper[1] presented the first comprehensive effort of this kind, based on certain approximations that have since been questioned by other workers[17,18] (see the discussion in the theory section).

0021-9673/89/$03.50

Although the treatment of Knox and Pyper cannot be regarded as quantitative, in our opinion their elegantly simple model still provides a clear and reliable guide for the better understanding and systematic optimization of preparative HPLC separations, which we hope to demonstrate here.

The work described here and in Part II[19] (based on the Craig model[3,4]) attempts to improve the accuracy of the Knox–Pyper treatment, and to further clarify various relationships that govern preparative HPLC when carried out under conditions that maximize the production rate P_R (grams per hour of purified product). A similar effort by Golshan-Shirazi and Guiochon[17,18] appeared when this study was completed, and a limited attempt has been made to compare our conclusions with those reported by them. Finally, it should be emphasized that other factors can limit the quantitative reliability of conclusions presented here and in their papers. Part III[20] examines one of these effects (variable column capacities for two compounds that are being separated).

THEORY

Knox–Pyper model

The treatment of preparative HPLC put forth by Knox and Pyper[1] predicts that elution bands will assume the shape of "nested right triangles" as the sample mass is increased, which is approximately the case in practice. Knox and Pyper then consider separation conditions such that two adjacent bands X and Y will just touch; this corresponds to the practical case where a maximum sample size is injected such that the recovery and purity of each component are 100%. This situation has been referred to as the "touching-band" case[6].

A number of simple relationships can be derived from this treatment[1,6], some of which are summarized in Table I (see the list of symbols at the end of the paper). Thus band width W can be predicted (eqns. 1–3) as a function of sample size, column capacity w_s and the chromatogram for a small-sample separation (values of the plate number N_0 and capacity factor k'). Likewise, the column capacity can be determined from a second run in which the sample size is large enough to result in some band broadening (eqn. 4). For every separation, an optimum value of the column plate number N_0 (for a small sample) is predicted, such that the production rate P_R is a maximum (eqns. 5–7). Finally, the maximum sample volume which will *not* affect the separation is given by eqn. 8.

The Knox–Pyper model ignores (a) the moderate departure of actual bands from right-triangular shapes, especially at higher loadings, and (b) the interaction of two adjacent (large-sample) bands during their migration through the column; *i.e.*, it is assumed that band migration for each solute proceeds independently of the presence of other compounds in the sample. As has been shown by Guiochon and co-workers (ref. 11 and later papers), actual separations under mass-overload conditions depart significantly from the simple picture of Knox and Pyper, especially for large plate numbers, small values of α and large samples. This is most strikingly exhibited in drastic changes in band shape, and the development of displacement boundaries between severely overlapping bands. However, practical chromatographers are primarily interested in the *results* of a preparative separation; which include production rate, recovery and purity of the desired product, that is, the way in which these quantities vary with experimental conditions, regardless of the contributing band

TABLE I

RELATIONSHIPS THAT CAN BE DERIVED FOR THE TOUCHING-BAND CASE (ASSUMES NESTED-RIGHT-TRIANGLE BANDS)

1 Band width W can be predicted as a function of sample size w, if the column capacity w_s is known[a], and a small-sample run (same conditions) has been carried out; for a compound Y, having a small-sample capacity factor k_y, retention time t_y, and plate number N_0, the band width W is given as

$$W = (4N_y)^{-1/2}\, t_y \tag{1}$$

where

$$N_y = N_0/[1 + (3/8)w_{xn}] \tag{2}$$

and

$$w_{xn} = N_0[k_y/(1 + k_y)]^2(w_y/w_s) \tag{3}$$

w_y is the weight of Y injected.

2 Column capacity w_s for a compound Y can be obtained from eqns. 1–3, by solving for w_s:

$$w_s = (3/8)\,[N_0N_y/(N_0 - N_y)]\,[k_y/(1 + k_y)]^2\, w_y \tag{4}$$

Thus a value of w_s can be obtained from a small-sample run (provides values of N_0, k_y) and a second run (same conditions) with a larger sample w_y (gives a value of N_y).

3 There is an optimum (small-sample) plate number N_{opt} for every touching-band separation:

$$N_{opt} = 16\, q\, [(1 + k_y)/k_y]^2\, [\alpha/(\alpha - 1)]^2 \tag{5}$$

where α is the separation factor (equal to k_y/k_x) and

$$q = N_y/N_0 \tag{6}$$

For a maximum production rate P_R, q will have a value of about 3. The quantity q can also be described in terms of the resolution of the corresponding small-sample separation R_s^0: $q = (R_s^0)^2$.

4 The sample size w_y for touching bands is given by

$$w_y = (w_s/6)[(\alpha - 1)/\alpha]^2[(q - 1)/q] \tag{7}$$

5 The sample volume V_s will not affect a touching-band separation, provided that

$$V_s < (1/2)F(t_y - t_x) \tag{8}$$

where F is the flow-rate (ml/min) and t_x and t_y are the retention times (min) of bands X and Y.

[a] w_s has also been referred to as the "saturation capacity" of the column, *i.e.*, the maximum weight of sample that can be held by the stationary phase.

shapes. It is this question that we propose to examine in this paper, using the concepts developed by Knox and Pyper[1] as a guide.

Craig simulations

We have shown that the Craig distribution is a reasonable model for the

chromatographic process under overload conditions. Experimental work reported by us is in good agreement with conclusions reached on the basis of the Craig model[3–6], and our general conclusions[6] match those of other workers who have approached preparative HPLC from different directions[1,21]. One limitation in our previous studies, however, is that the computer programs used by us were limited to separations that did not simultaneously involve heavily overloaded columns and/or large plate numbers. We have since extended our approach to allow simulations for any sample size, columns of any plate number and either isocratic or gradient elution.

The present computer program (CRAIG4) allows the simulation of any two-component separation. The general approach is similar to that described in refs. 4 and 22. The column is divided up into n_c equilibrium stages, with movement of the entire volume of mobile phase from one stage to the next during each transfer. The two-component Langmuir equations assumed here are given by eqns. 8 and 9 in ref. 4. This isotherm is numerically approximated by a new (modified compared with refs. 4 and 22) algorithm for approximating the distribution of a two-compound mixture between stationary and mobile phases in each Craig stage (described in the Appendix). This algorithm has been tested for various (artificial) two-component mixtures (values of k' and concentration varying for each component) *vs.* exact calculations from the two-component Langmuir model (by numerical means); our algorithm has been found to be accurate to within about $\pm 10\%$ for a wide range of sample concentrations and sample k' values. Other tests of the accuracy of this program (CRAIG4) will be offered below.

The present software provides simulations that can be expressed either graphically (*e.g.*, Fig. 1) or in table form (*e.g.*, Table II). We have found both formats to be useful. It should be noted that the number of stages n_c in these Craig simulations is equal to $N_0k'/(1 + k')$, *i.e.*, Craig stages are not the same as column plates[23].

RESULTS AND DISCUSSION

Verification of present Craig simulations

The present software was subjected to various tests to establish internal consistency; see the related discussion in refs. 3, 4 and 22. A rigorous computer model based on different principles to Craig simulation has been described by Ghodbane and

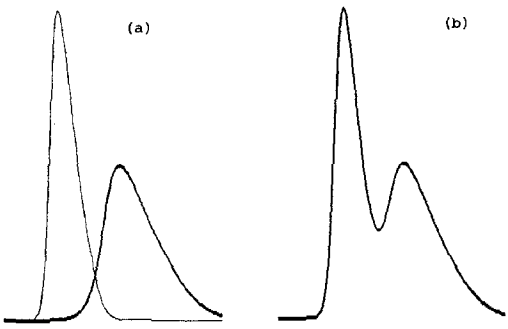

Fig. 1. Craig simulation (CRAIG4) for isocratic separation with following conditions: $k_x = 1$, $k_y = 1.7$, $w_x/w_s = w_y/w_s = 0.05$, $n_c = 100$ ($N_0 = 200$). (a) Individual solute bands; (b) composite chromatogram.

TABLE II

CRAIG4 OUTPUT (PARTIAL) FOR A SIMULATED SEPARATION WITH THE FOLLOWING CONDITIONS: $n_c = 100$ ($N_0 = 200$), $k_x = 1$, $k_y = 1.7$ ($\alpha = 1.7$), $w_x/w_s = w_y/w_s = 0.05$

Transfer No.	*Cumulative % eluted*[a]		*Purity in eluted fraction (%)*	
	X	*Y*	*X*	*Y*
⋮				
188	84.5	0.7 (99.3)	99.2	84.1
192	89.9	1.3 (98.7)	98.6	90.8
196	93.8	2.2 (97.8)	97.7	94.1
200	96.5	3.8 (96.2)	96.2	96.5
204	98.1	6.3 (93.7)	94.0	98.0
208	99.1	10.0 (90.0)	90.8	99.0
212	99.6	15.0 (85.0)	86.9	99.6
⋮				

[a] Numbers in parentheses refer to the recovery of *Y* in the second fraction; other values refer to the recovery of *X* or *Y* in the first fraction, eluted before the transfer number; *e.g.*, after 200 transfers, 96.5% of *X* has been eluted in this eluted fraction, the purity of *X* in this fraction is 96.2%, the amount of *Y* eluted is 3.8%, 96.2% of *Y* remains on the column and the purity of *Y* in the fraction following the first fraction is 96.5%.

Guiochon[11]; we shall compare certain predictions of the latter model with those given by our CRAIG4 program. Additionally, experimental data reported by us earlier[5] will be used as a further check on the accuracy of these Craig simulations.

CRAIG4 vs. Ghodbane and Guiochon model. We reported previously[6] that the Knox–Pyper treatment requires a correction factor of about 1.5-fold in sample size in order to match experimental results (band widths *W* and plate numbers *N*). A similar discrepancy was noted for comparisons of Craig with experimental data[3]. Further comparisons that suggest double the samples sizes in Craig simulation compared with experimental separations are reported in a later paper[24]. The model of Ghodbane and Guiochon has been shown[15] for several systems to provide good agreement with experimental data for a single-component sample as a function of sample size. Qualitative agreement with the latter model has also been demonstrated between theory and experiment for some two-component samples[20,25]. Therefore, if we wish to compare Craig simulations with the model of Ghodbane and Guiochon, it will be necessary to increase the sample size in the Craig simulations by a factor of 1.5–2.0 compared with those assumed in the Ghodbane and Guiochon model[a].

Ghodbane and Guiochon[14] reported results for several simulated separations that involve lower plate numbers ($797 < N_0 < 1645$). These separations are conveniently duplicated by Craig simulation, as the number of corresponding Craig

[a] A referee questioned whether errors in the isotherm that we have assumed (see Appendix) could account for the 1.5–2.0-fold error in predictions by Craig simulation. We consider this unlikely, as totally different numerical approximations to the Langmuir isotherm were used previously (polynomial fits[3,4]) and in the present Craig simulations (see Appendix), but each set of isotherms gives consistent results. Also, note that the 1.8-fold correction factor of Table II is constant over a wide range in separation conditions (including sample size). Finally, the factor 1.5 required in the Knox–Pyper model to achieve agreement with experiment is also suggestive of some more basic problem.

TABLE III

COMPARISON OF PREPARATIVE HPLC SEPARATIONS PREDICTED BY CRAIG4 *VS.* MODEL OF GHODBANE AND GUIOCHON[14]

Two-component sample A–B, with weight of B = three times that of A; $k_a = 4.6$, $k_b = 5.0$ ($\alpha = 1.09$); plate numbers as indicated.

Conditions	w/w_s[a]	*Predicted recovery of pure A or B (%)*[b]			
		Craig4		*Ref. 7*[c]	
		A	*B*	*A*	*B*
N_0 = 797, 98% pure A and B recovered	0.004	10	53	11	55
	0.010	7	45	7	47
	0.025	3	25	3	28
N_0 = 797, 95% pure A and B recovered	0.004	23	76	24	82
	0.010	18	73	19	74
	0.025	10	53	11	56
N_0 = 1055, 98% pure A and B recovered	0.004	23	67	24	63
	0.010	16	59	18	62
	0.025	7	31	8	34
N_0 = 1055, 95% pure A and B recovered	0.004	39	87	40	88
	0.010	32	82	34	84
	0.025	17	60	19	64

[a] Total sample weight divided by w_s.

[b] Recovery of material with indicated purity (95 or 98%).

[c] Predictions of Ghodbane and Guiochon model[14] for a sample that is 1.8-fold smaller than for CRAIG4 simulations (CRAIG4 sample size shown above).

stages is $n_c < 2000$, and computer run times are less than 16 h (IBM-AT with math coprocessor). Table III summarizes recovery data (for fractions of either 95% or 98% purity) for varying plate numbers and sample size, obtained from Figs. 3 and 4 in ref. 14. Corresponding predictions from CRAIG4 are also shown for comparison, based on a (best-fit) discrepancy in sample size of 1.8-fold. The overall agreement is $\pm 2\%$ (absolute) or $\pm 5\%$ (relative).

Another comparison of CRAIG4 with the Ghodbane and Guiochon model is shown in Fig. 2A and B for $N_0 = 1645$ and a (unadjusted) sample size of $w/w_s = 0.025$. The CRAIG4 sample size has been increased 1.8-fold ($w/w_s = 0.045$) for this comparison. Minor differences can be seen between the two simulations, but there is essential agreement in the overall shapes of the individual and composite bands.

CRAIG4 vs. experimental data. Fig. 2C and D compares experimental (Fig. 2D) and simulated (Fig. 2C) chromatograms for the separation of a mixture of two xanthines with a total sample size equal to 11% of the column capacity w_s. The sample size assumed in the Craig simulations was $1.8 \cdot 11\% = 20\%$ for this comparison; the other parameters (see Fig. 2C) were the same for both CRAIG4 and experimental runs. There is good agreement between these simulated and experimental results. Note also the sharp displacement front between the two bands (computer simulation, Fig. 2C). Further comparisons of experimental and simulated runs for mass-overloaded gradient elution are provided in another paper[24].

Assumptions. It should be recognized that the present Craig model assumes (1)

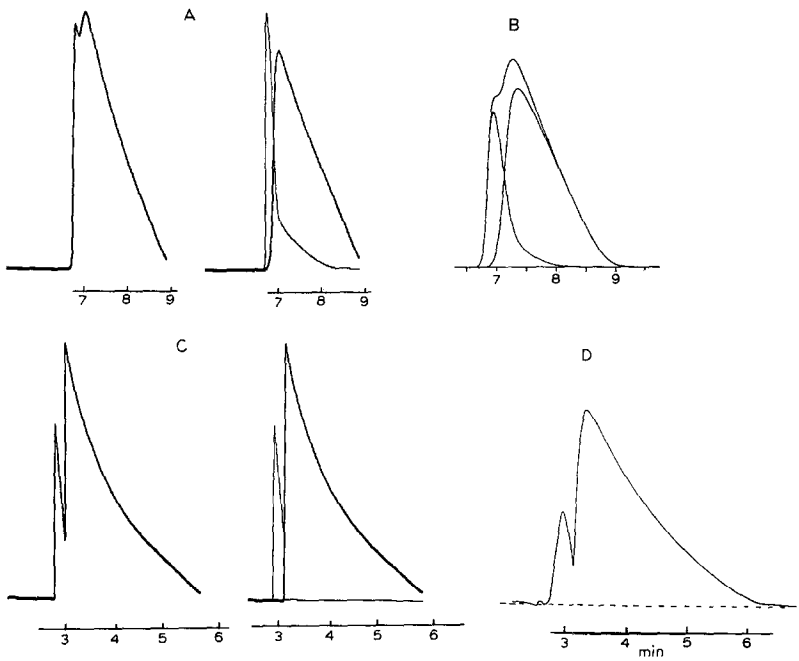

Fig. 2. Comparison of CRAIG4 simulations with model of Ghodbane and Guiochon[14] (A, B) and with an experimental separation (C, D). (A) CRAIG4 simulation for separation of sample in Table II; $N_0 = 1645$, $w/w_s = 0.045$ (B:A = 3:1); $k_a = 4.6$, $k_b = 5.0$; (B) same as (A) except for data in ref. 7 with $w/w_s = 0.025$; (C) CRAIG4 simulation for separation of sample with $N_0 = 5570$, $k_x = 1.85$, $k_y = 3.15$, $w/w_s = 0.20$; (D) experimental separation of two xanthines corresponding to separation (C) (ref. 14) with $w/w_s = 0.11$, 2.5 mg of hydroxyethyltheophylline (HET) and 25 mg of hydroxypropyltheophylline (HPT).

a Langmuir isotherm for each compound and mixtures thereof, and (2) equal w_s values for each compound in the mixture. These assumptions appear reasonable for typical samples, which consist of compounds of similar structure. However, many experimental separations appear to deviate significantly from this "ideal" behavior (see Part III[20]). The present discussion should therefore be regarded as semi-quantitative, rather than precise. The above 1.5–2.0-fold discrepancy in experimental *vs.* Craig-simulation sample sizes should also be kept in mind, although we have corrected for this discrepancy in final summaries reported here (*e.g.*, Figs. 9 and 11). Our objective in this study is to uncover general (if approximate) relationships for application to preparative HPLC, rather than to present precise equations for predicting preparative HPLC separations exactly.

Craig simulations

Simulations as a function of sample size were first carried out for a wide range of conditions: k' values for each component ($1 \leqslant k' \leqslant 6$), values of α ($1.2 \leqslant \alpha \leqslant 2$) and plate number N_0 ($20 \leqslant N_0 \leqslant 2000$). These studies were intended to provide an overall picture of separation under heavily overloaded conditions. Fig. 3 provides some typical results for the case of $k_x = 1.0$ and $k_y = 1.4$ ($\alpha = 1.4$), $N_0 = 800^a$, $w_x = w_y$ and

[a] The value of N_0 reported is always for the first band X. As a given number n_c of Craig stages is selected for each simulation, and as[23] $N_0 = (k' + 1)\, n_c/k'$, the value of N_0 for Y will always be slightly smaller. This was not corrected for in this study, but its effect on our final conclusions is not very significant.

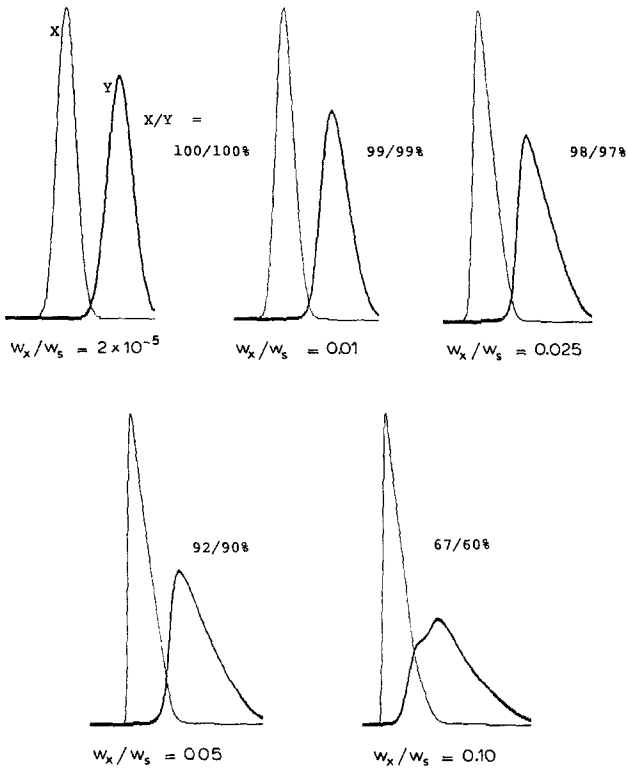

Fig. 3. Craig simulations showing effect of sample size on separation ($\alpha = 1.4$). Conditions: $k_x = 1, k_y = 1.4$, $n_c = 400$ ($N_0 = 800$).

different column loads. Chromatograms are shown for sample sizes w_x/w_s that vary from 0.00002 to 0.10. The quantity X/Y in Fig. 3 refers to the recovery of 99% pure product (X or Y) from the separation. Thus, for $X/Y = 92/90$, 92% of 99% pure X and 90% of 99% pure Y are recoverable in their separate fractions (as in Table I). Here and elsewhere we shall characterize the degree of separation achieved by the recovery of 99% pure product (values of X/Y); that is, we shall assume that the aim of the separation goal is the production of product of 99% purity. Guiochon and co-workers[12–14,17] presented data for the corresponding recoveries of less pure product (95% or 98% pure); see also the data in Table II.

Fig. 4 illustrates the effect of plate number N_0 on the separation in Fig. 3 for $w_x/w_s = 0.05$ or 0.10 ($50 < N_0 < 400$; $\alpha = 1.4$). An increase in N_0 increases the yield of 99% pure X and Y (X/Y%). Fig. 5 shows a similar series of separations to those in Fig. 3 (sample size varying), for a different value of α ($\alpha = 1.7$). The separations in Fig. 5 (for larger samples) are repeated in Fig. 6, but with varying ratios w_x/w_y. These latter chromatograms illustrate the compression of band X and the "tag-long" of band Y (caused by a large preceding band of X) discussed by Ghodbane and Guiochon[11,12].

Best conditions for maximum production rate

Experimental conditions (mobile phase, stationary phase) should first be

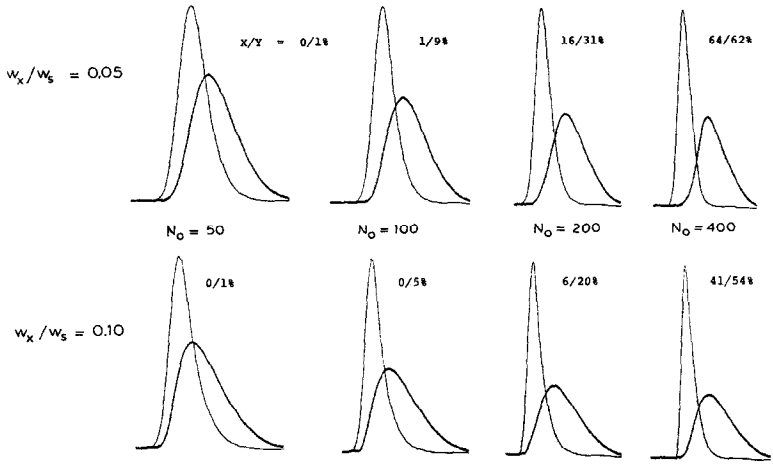

Fig. 4. Craig simulations showing effect of plate number N_0 on separation for two different sample sizes ($w_x/w_s = w_y/w_s = 0.05$ and 0.10); $k_x = 1$, $k_y = 1.4$.

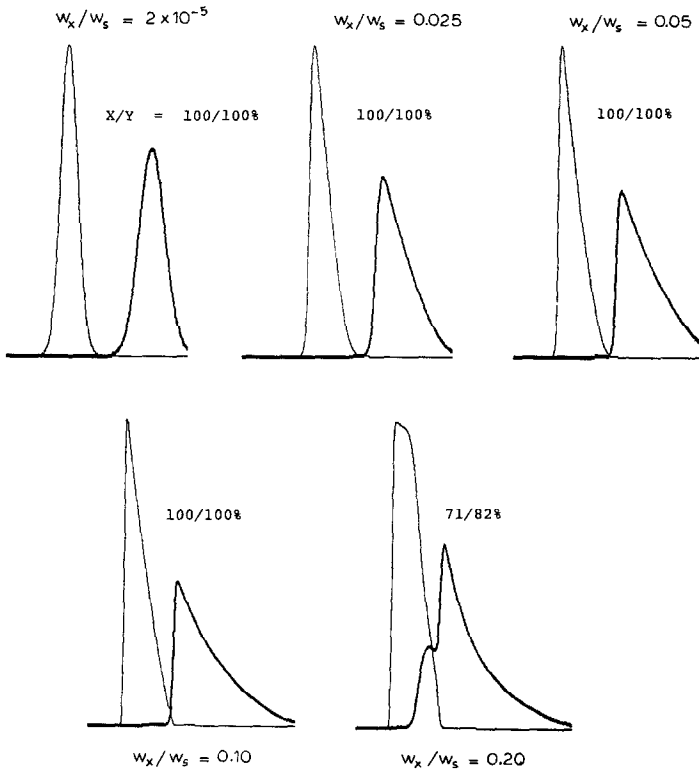

Fig. 5. Craig simulations showing effect of sample size on separation ($\alpha = 1.7$). Conditions: $k_x = 1, k_y = 1.7$. $n_c = 400$ ($N_0 = 800$).

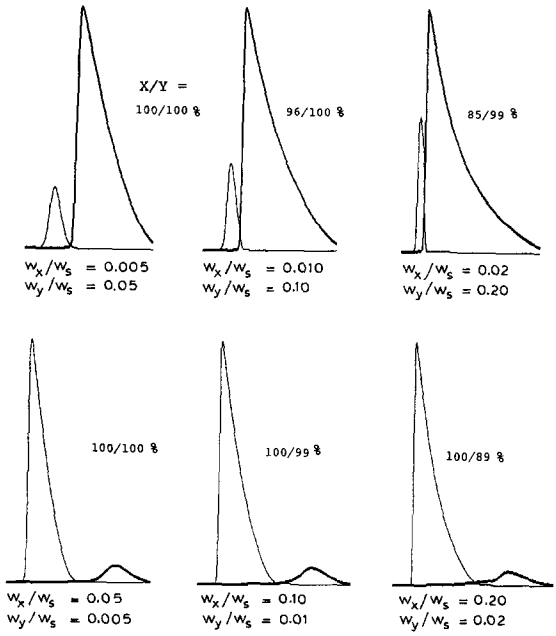

Fig. 6. Craig simulations showing effect of different relative concentrations of two components (X and Y). Conditions as in Fig. 6, except relative weights of X and Y differ.

selected for maximum values of α, as this variable is by far the most important in preparative HPLC[6]. In this study we assumed various values of α, then studied the effects on the production rate P_R of changes in k' (solvent strength), plate number (N_0) and sample size.

We also considered the production rate as a function of the recovery of purified product. In general, if we are willing to accept a lower recovery during each run, the production rate will be higher[12–14]. However, maximizing P_R without regard for product recovery (*i.e.*, accepting very low product recoveries) makes little economic sense. Usually there will be a substantial cost associated with reprocessing less pure product from a preceding HPLC run, and we assume that recoveries of less than 50% will rarely be acceptable. Therefore, we studied three different recovery levels: 50, 95 and 99.8% (touching bands).

Mapping production rate vs. plate number for different values of α. Our objective is to define conditions (sample size, k', N_0) for maximum production rate as a function of (a) different values of α and (b) the desired (or acceptable) recovery level (50–100%). This requires mapping P_R as a function of these variables. Our approach is illustrated in Fig. 7 for $\alpha = 1.7$, $k_x = 1.0$, and equal weights of X and Y in the sample[a]. Different sample sizes were selected ($w_x/w_s = w_y/w_s = 0.05$–0.40 in Fig. 7), and for each sample size separations were carried out with different values of N_0. Fig. 1 illustrates one such simulation, for $w_x/w_s = 0.05$ and $N_0 = 200$ ($n_c = 100$). Reference to Table II shows

[a] Later we shall discuss the effect of different values of w_x/w_y for the sample.

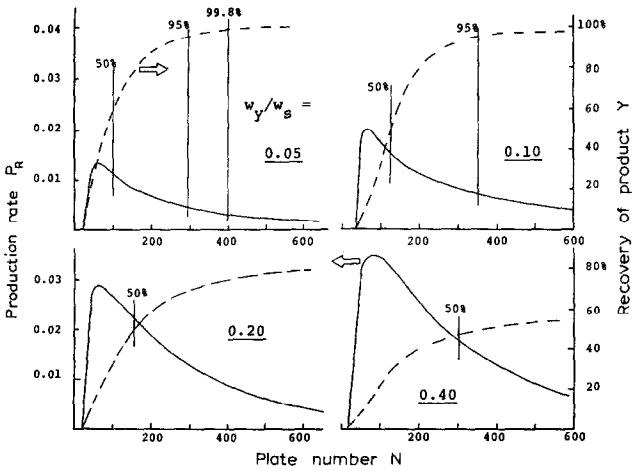

Fig. 7. Mapping production rate P_R (———) and recovery (– – –) of Y *vs.* column plate number N_0 for different sample sizes w_y/w_s; $k_x = 1$, $k_y = 1.7$, $w_x = w_y$.

that the recovery of 99% pure Y is equal to 90%. The production rate P_R was calculated (arbitrary units) to be equal to [(w_y/w_s) · (fractional recovery of Y)]/(run time)[a].

Production rate (solid lines) and recovery (dashed lines) were then plotted against N_0 as shown in Fig. 7 for different sample sizes (values of w_y/w_s). Vertical lines in Fig. 7 indicate the value of N_0 for recoveries of Y of 50, 95 and 99.8%. Thus, for a sample size $w_x/w_s = 0.05$, 50% recovery of Y in its 99% pure fraction corresponds to $N_0 = 100$; the production rate for this case is $P_R = 0.011$. For sufficiently large samples (*e.g.*, $w_x/w_s = 0.4$ in Fig. 7), it is not possible to recover 95% (or more) of Y in a 99% pure fraction; as N_0 is increased indefinitely, a limiting recovery is observed (about 60% for $w_y/w_s = 0.4$ in Fig. 7).

Determining the column plate number and sample size for maximum production rate (for a given recovery of Y). When the production rate and the recovery of Y have been mapped as in Fig. 7 for a given value of α, then P_R and the associated value of N_0 for a given recovery of Y can be plotted against sample size w_y/w_s. This is illustrated in Fig. 8 for the data in Fig. 7 ($\alpha = 1.7$). For a 50% recovery of Y, it is seen that a maximum production rate of 99% pure Y corresponds to values of $w_y/w_s = 0.25$ and $N_0 = 180$. Similarly, maximum production rates for recoveries of 95% and 99.8% of 99% pure Y correspond approximately to values of w_y/w_s and N_0 of 0.08 and 300 and of 0.07 and 600, respectively[b]. Because the optimum sample sizes are fairly similar for 95% and 99.8% recovery of Y, an average value of sample size *vs.* α for 95–100% recovery can be assumed.

---

[a] For $k_x = 1$ (as in the present example), the run time (retention time for Y) was defined as 1.0 for $N_0 = 100$; we assumed that run time is proportional to $N_0^{4/3}$ (corresponds to $n = 0.5$; see discussion in ref. 19). This assumes that the column pressure is held constant while varying the column length and flow-rate together to obtain the required value of N_0. Any resulting change in column length also changes w_s proportionately (taken into account here).

[b] These w_y/w_s values are Craig values; corresponding corrected values are $w_y w_s = 0.125$ (50% recovery), 0.04 (95% recovery) and 0.035 (99.8% recovery).

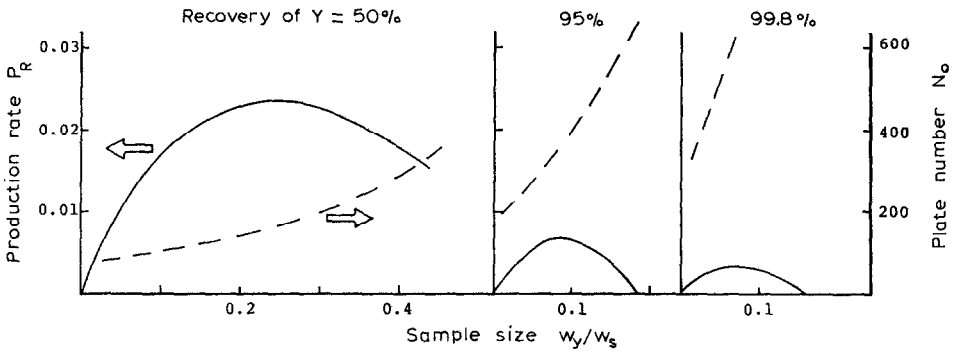

Fig. 8. Mapping production rate P_R and plate number N_0 *vs.* sample size for different recovery values for Y; $k_x = 1$, $k_y = 1.7$. Data from Fig. 7.

Values of w_y/w_s and N_0 for different combinations of α and recovery of Y (for maximum P_R) were determined in the same way (as illustrated in Figs. 7 and 8) for different values of k_x. For the moment, we shall restrict our discussion to the case where $k_x = 1$. Figs. 9 and 10 summarize these results, as plots of sample size and plate number *vs.* α, for different recoveries of Y (assuming equal amounts of X and Y in the sample). Given a value of α from an optimized analytical separation, and some desired recovery of Y in each run, Figs. 9 and 10 can be used to determine the appropriate values of N_0 and w_y/w_s for a maximum production rate. This is conceptually similar to the Knox–Pyper approach as summarized in Table I. The dashed curve in Fig. 9 is the sample size predicted by Knox and Pyper (Table I). It is in error (compared with the "99.8% recovery" curve) by a factor of about 2, owing to the failure to recognize sample interaction.

Sample size and production rate. Fig. 11 is a plot of production rate for the optimum conditions summarized in Figs. 9 and 10. It is apparent from Fig. 11 that a significant increase in production rate is possible by the use of larger samples than

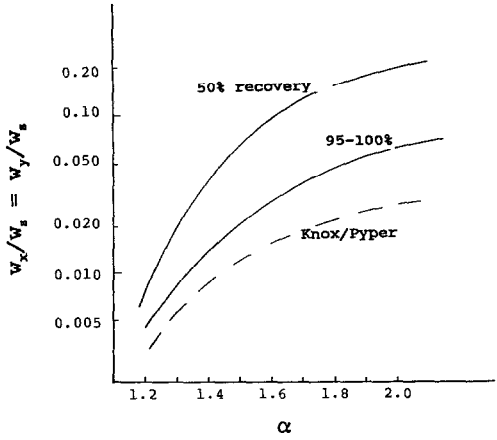

Fig. 9. Optimum sample sizes for maximum production rate and various values of α and recovery of pure Y. Derived from Craig simulations as in Figs. 7 and 8 for $k_x = 1$ and $w_x = w_y$.

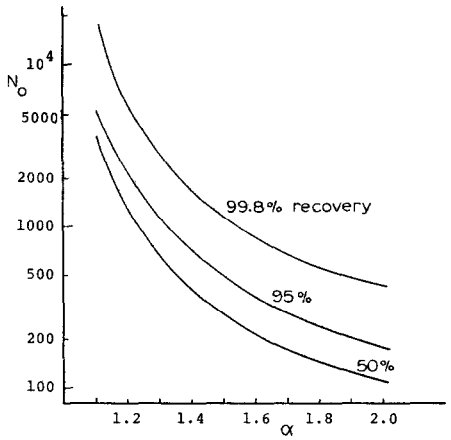

Fig. 10. Optimum plate number for maximum production rate and various values of α and recovery of pure *Y*. Derived from Craig simulations as in Figs. 7 and 8 for $k_x = 1$ and $w_x = w_y$.

correspond to "touching bands" (99.8% recovery in Fig. 11). Recoveries of 95% or 50% allow increases in P_R (compared with the touching-band case) of about 3-fold (95%) and 10-fold (50%), respectively. There is only a limited advantage in terms of production rate in accepting recoveries of pure *Y* less than 50%, especially for $\alpha > 1.5$.

Illustration of Figs. 9 and 10. Fig. 12 summarizes some chromatograms (both individual band and composite) obtained for various values of α and recovery of *Y*, based on the optimized sample size and plate number data in Figs. 9 and 10. The

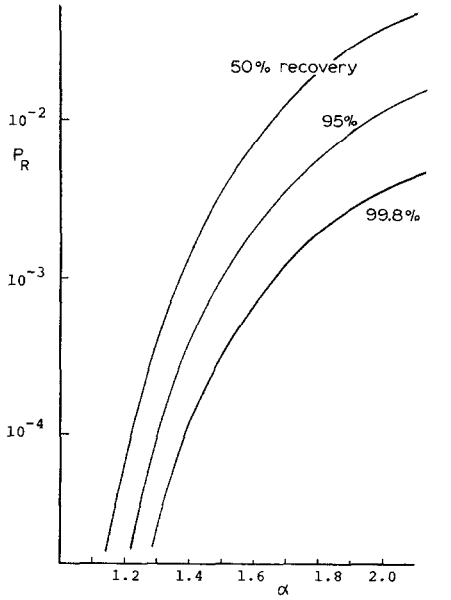

Fig. 11. Maximum production rates for different values of α and recovery of *Y*, corresponding to conditions in Figs. 9 and 10 ($k_x = 1$, $w_x = w_y$).

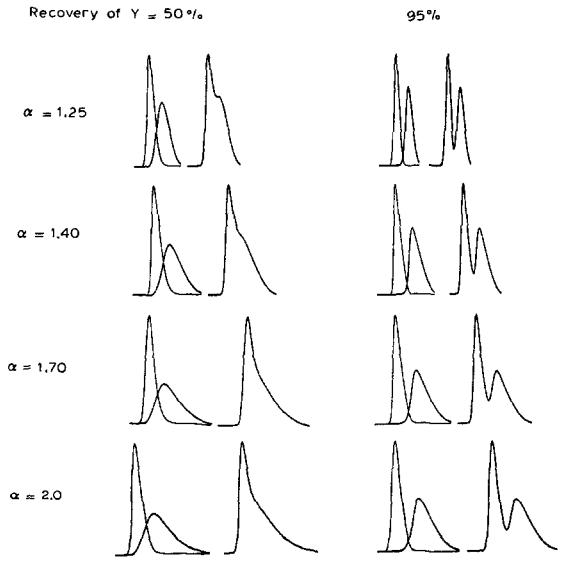

Fig. 12. Craig simulations for optimum conditions from Figs. 9 and 10 (for maximum P_R); $k_x = 1$, $w_x = w_y$.

appearances of the chromatograms in Fig. 12 are generally similar for similar recoveries, suggesting that visual comparisons of actual runs (under overload conditions) with the examples in Fig. 12 (or Fig. 13, for $k_x = 3$) can be used to calculate the possible recovery of pure product from a given run. Note also that it is possible to calculate cut-points (approximately) for the collection of pure product from these examples.

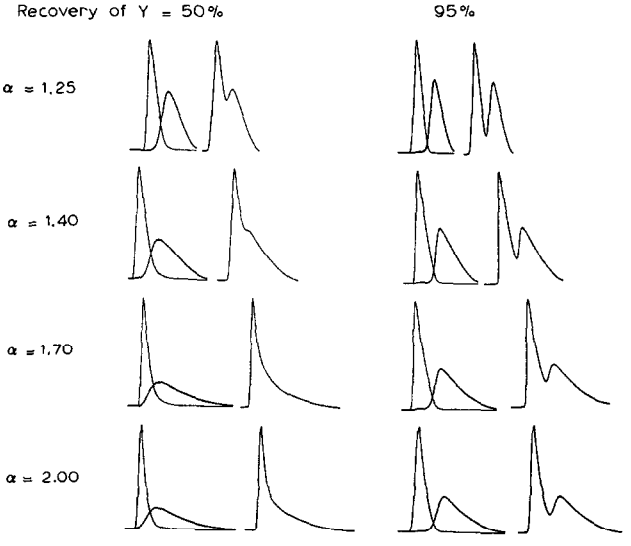

Fig. 13. Craig simulations as in Fig. 12, except $k_x = 3$. See text for details.

Effect of k'. The procedure outlined in Figs. 7–11 was repeated for different values of k_x ($0.5 \leqslant k_x \leqslant 3$). The conclusions of this study are as follows:

(1) the optimum values of w_y/w_x are about the same as for $k_x = 1$ (see Fig. 9), depending on α and the recovery of Y;

(2) the optimum values of N_0 decrease for increasing k_x; *e.g.*, for $\alpha = 1.7$, $N_0 = 660$ (for $k_x = 0.5$), 300 ($k_x = 1$), 190 ($k_x = 2$) and 130 ($k_x = 3$);

(3) P_R changes by less than 10% for $0.5 \leqslant k' \leqslant 3$, with $k' = 1$ being the optimum value.

Fig. 13 summarizes a number of simulations (as in Fig. 12) for $k_x = 3$, for the purpose of illustrating the predicted separations.

Effect of α. The separation factor α is of critical importance for maximum production rate in preparative HPLC. Fig. 14 is a log–log plot of the data in Fig. 12 in the form of production rate *vs.* $(\alpha - 1)$. The lines each have a slope of 3, meaning that $P_R \approx$ (constant) $\cdot (\alpha - 1)^3$ (ref. 3). Golshan-Shirazi and Guiochon[18] reported a lesser dependence of production rate on α, but this seems to reflect a different approach to optimizing the production rate. It is not clear whether these workers considered the dependence of the required plate number N_0 on α, and the related dependence of N_0 on the time of separation.

Applicabilty of the Knox–Pyper model to the preceding data. Now that we have mapped values of N_0 for maximum production rate *vs.* k' and α, it is interesting to compare our conclusions with those of Knox and Pyper[1], as summarized in eqns. 5 and 7 (Table I). These relationships indicate that production rate can be maximized by selecting particular values of sample size and column plate number N_0 (N_{opt} in eqn. 5) for the case of "touching-band" separation. The value of N_{opt} is further dependent on values of k' (k_y) and α. The above discussion (Figs. 9–11) shows that this is also true of more heavily overloaded separations, such that the recovery of pure product is less

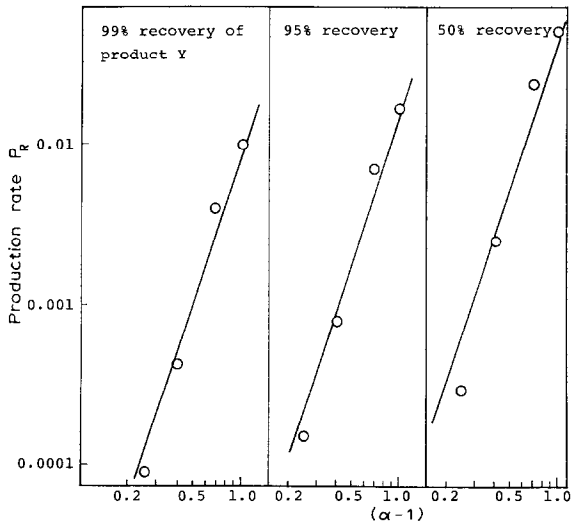

Fig. 14. Dependence of production rate on the separation factor α for $k_x = 1$ and $w_x = w_y$.

than 100% (50–99.8%), that is, there is an optimum value of N_0 for maximum production rate, and this value of N_0 varies with k' and α.

Eqn. 5 can be better appreciated by recognizing that the factor q in this equation is related to the resolution R_s of the small-sample separation that corresponds to the desired preparative separation. Thus, in the treatment of Knox and Pyper[1], q is the ratio of plate numbers (N_0/N) for the small-sample *vs.* touching-band separation. Resolution can be expressed as

$$R_s = (1/4)\,(\alpha - 1)\,N_0^{1/2}\,[k'/(k' + 1)] \tag{9}$$

from which it is seen that (only N_0 varies)

$$q = [(R_s^0)/R_s]^{1/2} \tag{10}$$

where, R_s^0 is the resolution of the small-sample separation and R_s is that of the preparative separation (optimized for maximum production rate). For "touching-band" separations as defined in ref. 1, $R_s = 1$, so that $q = (R_s^0)^{1/2}$ for this case. Knox and Pyper[1] proposed $q = 3$ as an optimum value, whereas we have suggested[6] that $q = 2.5$ is more likely[a].

The treatment of Knox and Pyper[1] for touching-band separations therefore suggests that the optimum value of N_0 for a touching-band separation (100% recovery) corresponds to a small-sample resolution of the two bands equal to $(2.5\text{–}3.0)^{1/2} = 1.6\text{–}1.7$. That is, regardless of the values of k' and α for the small-sample separation, the plate number N_0 should be adjusted to give $R_s \approx 1.6$ for a small sample. We shall next extend this important generalization to the case of more heavily overloaded separations, such that the recovery of pure product is less than 100%.

As the sample loading is increased, the resolution R_s of the final separation will decrease. If $q = 2.5$ is a generally optimum value, N_0 and R_s^0 must also decrease for maximum production rate (eqn. 10). The simulations we have carried out and summarized in Figs. 9–11 allow us to check this hypothesis. For a 50% recovery of pure product, we find that $R_s^0 = 0.91 \pm 0.07$ (1 S.D.) for $k_x = 1$ and $1.25 < \alpha < 2.0$. Similarly, for $k_x = 3$, $R_s^0 = 0.88$ (fewer data points available). That is, the initial adjustment of column plate number to give a small-sample resolution $R_s^0 = 0.9$ provides an (approximately) optimum value of N_0 for maximum production rate (50% recovery, regardless of the (small-sample) values of k' and α. Eqn. 10 also indicates that the resolution of the overloaded run (providing 50% recovery of pure product) will be $R_s = 0.9/(2.5)^{1/2} = 0.6$. Examination of the corresponding separations in Figs. 12 and 13 shows reasonable agreement with this prediction (*cf.*, standard resolution curves in ref. 26).

A similar examination of the data reviewed here (Figs. 9–11 plus data for $k_x = 3$) shows for a 95% recovery of pure product that the optimum value of R_s^0 is 1.18 ± 0.06, or the resolution of the overloaded run should be $R_s \approx 0.8$ (eqn. 10 with $q = 2.5$; again, compare Figs. 12 and 13 with standard resolution curves). Finally, the optimum value

[a] Our analysis of ref. 6 shows that q is related to the coefficient n in ref. 19: $q = 2 + n$. In this paper we assume that $n = 0.5$. The data in Figs. 9–11 are also based on a value of $n = 0.5$ (or $q = 2.5$).

of R_s^0 for 99.8% recovery is 1.8. (*cf.*, the Knox–Pyper prediction of 1.6–1.7).

To summarize, our extension here of the Knox–Pyper relationship (eqn. 5) seems to provide a clear and simple picture of the interrelationship of optimum values of N_0 with experimental conditions (values of k' and α) and the desired recovery of pure product. Depending on the desired recovery of pure product, selecting a value of N_0 that yields a certain small-sample resolution R_s^0 will provide a maximum production rate, regardless of the values of k_x or α.

Recovery of X. The preceding discussion and Figs. 7–11 concern only the recovery of the second band Y from the separation of a mixture of X and Y. The recovery of X parallels that of Y, but with some differences as summarized in Table IV. Here the corresponding recoveries of X are shown for either a 50% or 95% recovery of Y, as a function of α and k_x. The recovery of X tends to be greater than that of Y for low values of α, and higher for large α. For recoveries of $Y > 95\%$, the recoveries of X and Y are the same.

Effect of varying concentrations of product and impurities. Figs. 5 and 6 illustrate the general effect of changes in the relative concentrations of X and Y on the separation. The recovery of 99% pure X or Y increases (for the same weight of X plus Y) as its relative concentration in the sample increases. This is also shown by the examples in Fig. 15. Here, a comparison is made with an optimized run for $\alpha = 1.7$, $k_x = 1$, $w_x = w_y$ and a 95% recovery of pure Y (top example). Relative to this starting case, the relative concentrations of X and Y are varied by 1:10 and 10:1 (lower examples in Fig. 15). The series labeled 1–X have the same sample size of the major band as in the "optimized run" ($w/w_s = 0.095$), while the series labeled 1/4–X have a sample size that is one quarter as great (0.024), and the series labeled 4–X have a sample size that is four times greater.

Several conclusions can be drawn from the examples in Fig. 15:

(1) When one component of the sample is present in greater concentration than adjacent minor bands (ten times greater in Fig. 15), a larger weight of the major band can be separated (other conditions remaining the same), with an equivalent recovery of purified product (95% in this example). For a concentration of the minor band equal to 10% of the major band concentration, about four times as much of the major band

TABLE IV

RECOVERY OF 99% PURE X COMPARED WITH THAT OF Y

k_x	α	*Recovery of band X (%)*	
		Recovery of Y = 50%	*Recovery of Y = 95%*
1	1.25	58	95
	1.40	50	95
	1.70	26	93
	2.00	22	93
3	1.25	60	94
	1.40	43	96
	1.70	30	94
	2.00	28	93

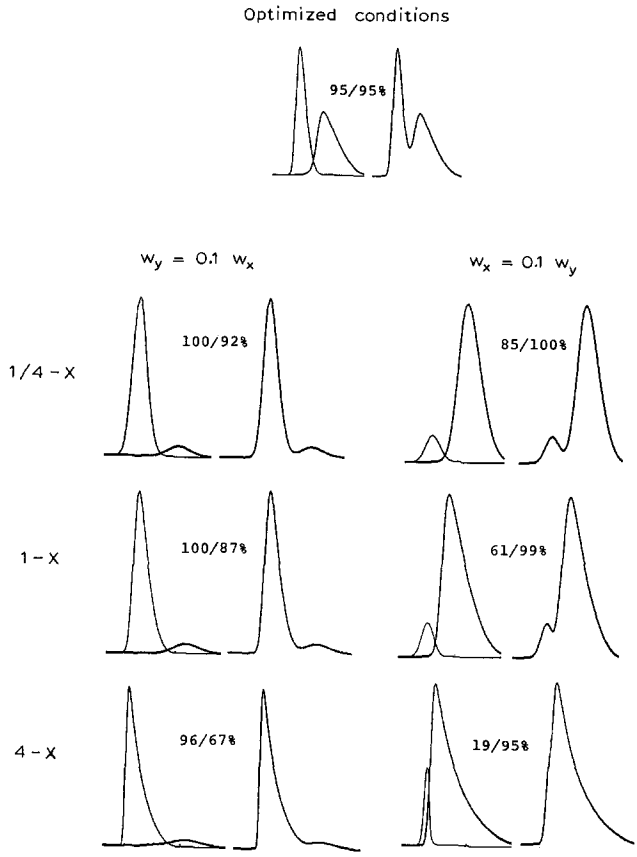

Fig. 15. Craig simulations for two sample components that are present in different concentrations. Conditions: $N_0 = 400$, weight of major band $= w/w_s = 0.095$, $k_x = 1$, $k_y = 1.7$ ($\alpha = 1.7$). Separation for "optimized conditions" (top) has $w_x = w_y$. Other separations have a 10-fold difference in the concentrations of X and Y. Values in figure (*e.g.*, 95/95%) refer to recovery of X and Y at 99% purity. Weight of major band in "1/4–X" runs is (0.095/4) = 0.024; weight of major band in "4–X" runs is (0.095 · 4) = 0.38.

can be separated per run, with the same purity and recovery (99% and 95% here).

(2) Conversely, the recovery and/or purity of a minor fraction will be lower. In the examples in Fig. 15, a 95% recovery of 99% pure impurity is not even possible.

(3) The best strategy for maximizing P_R for the minor bands in Fig. 15 is to charge a 4–X sample, collect 95% of the minor band and reseparate the total fraction (one run) under the same conditions. For the examples in Fig. 14, a 95% recovery of 99% pure minor component is possible in this way.

(4) It is also seen that a better recovery occurs of a minor band that elutes later rather than earlier, *e.g.*, a 67% recovery of 99% pure material in the 4–X example in Fig. 14 compared with 19% when the minor band elutes earlier.

CONCLUSIONS

Table I outlines a number of general conclusions concerning the selection of optimum conditions for the maximum production rate of purified product, as derived from the simple Knox–Pyper model. These rules remain qualitatively unchanged when the sample size is increased into the heavily overloaded region. Thus, for every separation there will be an optimum value of N_0, which is determined by values of α, k_x and the desired recovery of product. The use of either larger or smaller values of N_0 will result in a decrease in the possible production rate. The plots in Fig. 8 show, however, that values of P_R are not highly sensitive to the exact value of N_0 chosen. A change in N_0 by $\pm 50\%$ is not very significant (± 10–20% change in production rate), provided that the sample size is adjusted to maintain the desired recovery of Y, *i.e.*, larger samples for larger values of N_0 and smaller samples for smaller N_0 values.

The optimum value of N_0 for a given preparative separation can be estimated from the small-sample separation. The column plate number should be adjusted so that the resolution (R_s^0) of the corresponding small-sample separation equals about 0.9 for a 50% recovery of pure product, about 1.2 for 95% recovery and 1.7 for 99.8% recovery. These observations represent a straightforward extrapolation of recommendations put forth by Knox and Pyper[1].

Another conclusion from this study is that a maximum production rate is favored by a k' value for band X (k_x) of about 1[a]. However, P_R changes by less than 10% for $0.5 \leqslant k_x \leqslant 3$. However, if the solvent recovery costs are a major part of the total purification costs, lower values of k_y will be economically favored despite some decrease in P_R.

Part III[20] discusses an additional feature of these overlapping-band separations, namely differences in column capacity values (w_s) for two adjacent bands in the chromatogram (X and Y). When this occurs, it can have a major effect on the optimum sample size and production rate. In view of this resulting complication, attempts at the precise optimization of preparative HPLC separations are probably premature at present. For the moment, it seems more important to seek a semi-quantitative description of these separations that can be used to guide the (necessarily) trial-and-error development of final preparative HPLC procedures.

APPENDIX

Algorithm for calculating the distributon of two compounds X and Y in a Langmuir-type system as a function of the total weights of X and Y in the combined mobile and stationary phases

A one-stage equilibrium is assumed, having a mobile-phase volume of 1.0 ml and a stationary phase capacity of 0.1 g of sample. The weights of X and Y in the mobile (m) and stationary (s) phases are w_{xm}, w_{xs}, w_{ym} and w_{ys}. The total weights w_x and w_y of X and Y in the stage are known. The capacity factors of X and Y (small sample) are k_x and k_y. The following derived quantities are first calculated for specified values of k_x and k_y:

---

[a] This assumes that α does not vary as the solvent strength is changed. If α changes with k', then a larger value of k' will be optimum in terms of production rate (and *vice versa*, if α decreases with k').

$$\alpha = k_y/k_x$$
$$D_x = (0.5/k_x) + 0.7\,k_x^{0.37}$$
$$D_y = (0.5/k_y) + 0.7\,k_y^{0.37}$$
$$C_x = 0.62\,10^{D_x}k_x^{-0.4}$$
$$C_y = 0.62\,10^{D_y}k_y^{-0.4}$$
$$w_{max} = 0.175 - 0.013 \log k_x$$
$$w_{tot} = w_x + w_y$$

We first compare w_{tot} with w_{max}: if $w_{tot} > w_{max}$, see procedure A. If w_{tot} is not $> w_{max}$, see procedure B.

Procedure A. Check to see if w_x or $w_y = 0$; if so,

for $w_x = 0$, $w_{ys} = 0.1$, $w_{ym} = 0.1 - w_y$;
for $w_y = 0$, $w_{xs} = 0.1$, $w_{xm} = 0.1 - w_x$.

If neither w_x or $w_y = 0$, then

$$Q = w_x + w_y - 0.1$$
$$A = 1 - \alpha$$
$$B = [w_x(\alpha - 1)] + 0.1\alpha Q$$
$$C = -w_x\alpha Q$$
$$w_{xm} = [-B + (B^2 - 4AC)^{1/2}]/2A$$
$$w_{xs} = w_x - w_{xm}$$
$$w_{ys} = 0.1 - w_{xs}$$
$$w_{ym} = w_y - w_{ys}$$

Procedure B.

$$J_x = w_x + (\alpha^{1/2}w_y)w_y$$
$$J_y = w_y + (\alpha^{-1/2}w_x)w_x$$
$$R_x = (1/k_x) + C_xJ_x^{Dx}$$
$$R_y = (1/k_y) + C_yJ_y^{Dy}$$
$$W_{xs} = w_x/(1 + R_x)$$
$$w_{xm} = w_x - w_{xs}$$
$$w_{ys} = w_y/(1 + R_y)$$
$$w_{ym} = w_y - w_{yx}$$

SYMBOLS (PARTS I–III)

Reference to equations or figures in the various papers in this series is identified by use of I-, II- or III; *e.g.*, eqn. III-3 refers to eqn. 3 in Part III.

A, B, C	coefficients (constant for a given system) in the Knox equation (eqn. II-3)
b_x, b_y	Langmuir coefficients for X and Y (eqns. III-4 and -5)
C_x, C_y	concentrations of X and Y in mobile phase (mole fractions)
d_c	column inside diameter (cm)
D_m	solute diffusion coefficient (cm^2/s)
d_p	column-packing particle diameter (μm)

F	flow-rate (ml/min)
h	reduced plate height (eqn. II-3)
H	plate height $= L/N_0$
k'	solute capacity factor
k_0	value of k' for a small sample
k_y	value of k_0 for solute Y
K	Equilibrium constant (eqn. III-2)
L	column length (cm)
m, s	mobile and stationary phases
M	solute molecular weight
n	parameter which relates values of N_0 to flow-rate, equal to d(log h)/d(log v) (eqn. II-6 and Table II-1)
n_c	number of Craig stages in a computer simulation; $n_c = [k'/(1 + k')]N_0$
N_y	column plate number for a large sample of Y (eqn. I-2)
N_0	value of N for a small sample; in computer simulations, $N_0 = (1 + k')n_c/k'$
N_{opt}	optimum value of N_0 for a preparative HPLC separation (eqn. I-5)
P	column pressure (p.s.i.)
P_R	production rate (mg/h of purified product)
q	column efficiency parameter (eqn. I-6)
R_s	resolution of preparative separation
R_s^0	resolution of small-sample separation
SA	stationary phase surface area for a column (m^2)
t_0	column dead-time (min)
t_R^0	retention time (min) for a small sample; also, run-time (eqn. II-1)
t_x, t_y	value of t_R^0 for solutes X or Y (min)
v	constant defined by eqn. II-11
V_m	column dead-volume (ml)
V_s	maximum volume of injected sample that will not affect a preparative separation (ml) (eqn. I-8)
w	total weight of injected sample; usually combined weights of X and Y (mg)
w, x, y, z	constants defined by eqn. II-7
w_s	column saturation capacity (mg)
w_{sx}, w_{sy}	w_s values for X and Y (mg)
w_x	weight of solute X injected onto the column (mg)
w_{xn}	eqn. I-3
w_{xs}	weight of solute in stationary phase (mg)
w_y	weight of solute Y injected onto the column (mg)
W	baseline band width (min); see Figs. 2 and 3
W_0	value of W for a small sample
x, y	subscripts referring to bands X and Y
X, Y	adjacent sample bands; Y corresponds to the desired product and X is the preceding band
α	separation factor for two solutes
v	mobile phase reduced velocity (eqn. II-5)
θ_x, θ_y	mole fraction of X or Y in the stationary phase; normally assumes equal numbers of X, Y or mobile phase molecules in a saturated monolayer

REFERENCES

1 J. H. Knox and H. M. Pyper, *J. Chromatogr.*, 363 (1986) 1.
2 A. Jaulmes, C. Vidal-Madjar, H. Colin and G. Guiochon, *J. Phys. Chem.*, 90 (1986) 207.
3 J. E. Eble, R. L. Grob, P. E. Antle and L. R. Snyder, *J. Chromatogr.*, 384 (1987) 25 and 45.
4 J. E. Eble, R. L. Grob, P. E. Antle and L. R. Snyder, *J. Chromatogr.*, 405 (1987) 1.
5 J. E. Eble, R. L. Grob, P. E. Antle, G. B. Cox and L. R. Snyder, *J. Chromatogr.*, 405 (1987) 31.
6 L. R. Snyder, G. B. Cox and P. E. Antle, *Chromatographia*, 24 (1987) 82.
7 G. Guiochon, S. Golshan-Shirazi and A. Jaulmes, *Anal. Chem.*, 60 (1988) 1856.
8 S. Golshan-Shirazi and G. Guiochon, *Anal. Chem.*, 60 (1988) 2364.
9 S. Golshan-Shirazi, S. Ghodbane and G. Guiochon, *Anal. Chem.*, 60 (1988) 2630.
10 S. Golshan-Shirazi and G. Guiochon, *Anal. Chem.*, 60 (1988) 2634.
11 S. Ghodbane and G. Guiochon, *J. Chromatogr.*, 440 (1988) 9.
12 S. Ghodbane and G. Guiochon, *J. Chromatogr.*, 444 (1988) 275.
13 S. Ghodbane and G. Guiochon, *J. Chromatogr.*, 450 (1988) 27.
14 S. Ghodbane and G. Guiochon, *J. Chromatogr.*, 452 (1988) 209.
15 S. Golshan-Shirazi and G. Guiochon, *Anal. Chem.*, 61 (1988) 462.
16 A. Katti and G. Guiochon, *Anal. Chem.*, 61 (1989) 982.
17 S. Golshan-Shirazi and G. Guiochon, *Anal. Chem.*, 61 (1989) 1267.
18 S. Golshan-Shirazi and G. Guiochon, *Anal. Chem.*, 61 (1989) 1368.
19 L. R. Snyder and G. B. Cox, *J. Chromatogr.*, 483 (1989) 85.
20 L. R. Snyder and G. B. Cox, *J. Chromatogr.*, 483 (1989) 95.
21 H. Poppe and J. C. Kraak, *J. Chromatogr.*, 255 (1983) 395.
22 L. R. Snyder, G. B. Cox and P. E. Antle, *J. Chromatogr.*, 444 (1989) 303.
23 B. L. Karger, L. R. Snyder and Cs. Horvath, *An Introduction to Separation Science*, Wiley-Interscience, New York, 1973, pp. 110–116.
24 G. B. Cox, L. R. Snyder and J. W. Dolan, *J. Chromatogr.*, 484 (1989) 409.
25 J. Newburger and G. Guiochon, *J. Chromatogr.*, 484 (1989) 153.
26 L. R. Snyder and J. J. Kirkland, *Introduction to Modern Liquid Chromatography*, 2nd ed., Wiley-Interscience, New York, 1979, pp. 38–40.